Multiphoton-Excited Serotonin Photochemistry

Michael L. Gostkowski, Richard Allen, Matthew L. Plenert, Eric Okerberg, Mary Jane Gordon, and Jason B. Shear

Department of Chemistry and Biochemistry, The Institute for Cellular and Molecular Biology, and The Center for Nano and Molecular Science and Technology, The University of Texas, Austin, Texas

ABSTRACT We report photochemical and photophysical studies of a multiphoton-excited reaction of serotonin that previously has been shown to generate a photoproduct capable of emitting broadly in the visible spectral region. The current studies demonstrate that absorption of near-infrared light by an intermediate state prepared via three-photon absorption enhances the photoproduct formation yield, with the largest action cross sections ($\sim 10^{-19}$ cm^2) observed at the short-wavelength limit of the titanium:sapphire excitation source. The intermediate state is shown to persist for at least tens of nanoseconds and likely to be different from a previously reported oxygen-sensitive intermediate. In addition, the two-photon fluorescence action spectrum for the fluorescent photoproduct was determined and found to have a maximum at ~780 nm (3.2 eV). A general mechanism for this photochemical process is proposed.

INTRODUCTION

Characterization of biological molecules using their intrinsic fluorescence properties circumvents artifacts caused by fluorescence labeling and, as a consequence, has been a useful approach for examining phenomena ranging from protein folding to neurotransmitter packaging. Nevertheless, such analyses can be severely limited by the poor photophysical and photochemical properties of ultraviolet (UV) excitable chromophores such as tryptophan, tyrosine, and the monoamine neurotransmitters.

As an alternative to conventional fluorescence approaches, multiphoton-excited (MPE) fluorescence has provided improved capabilities to measure small quantities of biological molecules in microscopy and spectroscopy, primarily because background from scatter and instrument autofluorescence can be virtually eliminated by using near-infrared (NIR) light in place of UV excitation. Webb and co-workers, for example, demonstrated that UV fluorescence from cellular serotonin (5-hydroxytryptamine, 5HT) granules could be imaged via three-photon excitation (Maiti et al., 1997). Unfortunately, photobleaching quantum yields generally are at least as large for nonlinear excitation as they are for single-photon excitation (1PE) (Patterson and Piston, 2000). Several reports have shown that enhanced photodegradation of synthetic and biological chromophores can be caused by higher-order photonic events, with three- and four-photon-promoted photobleaching accompanying two-photon-excited fluorescence (Chen et al., 2002; Patterson and Piston, 2000; Springer and Higgins, 2000). Although specific photochemical mechanisms typically have not been elucidated, it has been suggested that bleaching efficiencies may be enhanced by NIR absorption from various excited states (Chen et al., 2002; Patterson and Piston, 2000).

Multiphoton-excited photochemistry of 5HT presents a particularly interesting system for study. Previously, 5HT was shown to undergo a four-photon-excited phototransformation process, forming a product that could be excited to fluoresce ($\lambda_{max,em} \approx 500$ nm) via absorption of two additional photons (Shear et al., 1997). This photoderivatization process has been exploited to improve 5HT detectability in low-volume capillary electrophoresis (CE) assays severalfold relative to measurements based on intrinsic UV fluorescence (Gostkowski et al., 1998b, 2000). Fluorescent 5HT photoproduct forms in several microseconds or less and degrades rapidly, probably within tens of milliseconds (Gordon and Shear, 2001). Although several studies have investigated cosolute effects on generation of 500-nm emission in solutions of 5-hydroxyindoles (Shear et al., 1997; Gostkowski et al., 2000; Bisby et al., 2003), such studies have yet to define the specific mechanisms by which these molecules undergo phototransformation.

Recently, Bisby and co-workers reported that a photoproduct with similar emission properties could be generated from 5-hydroxytryptophan (5HTrp) using a pulsed 308-nm XeCl laser (Bisby et al., 2003). Product fluorescence could be excited using the same laser or could be elicited at varying intervals after the XeCl pulse using a pulsed 430-nm dye laser. The visible-emitting product was reported to have unusual, two-step formation kinetics: a brief (<10 ns) phase that led to nearly 50% of the measured visible emission, followed by a long exponential formation period ($\tau \approx 3.5$ μs). It is unclear how many 308-nm photons are necessary to promote photoreaction or whether the resultant visible-emitting product(s) is identical to that which is formed using pulsed NIR light.

Here, we report findings of pump-probe experiments that provide insights into the mechanisms by which 5HT undergoes multiphoton-excited transformation to a visible-emitting product. A reaction intermediate prepared via three-photon excitation is shown to be capable of absorbing

Submitted August 18, 2003, and accepted for publication December 2, 2003.

Address reprint requests to Jason B. Shear, University of Texas, Chemistry and Biochemistry, 1 University Station A5300, Dept. of Chemistry, Austin, TX 78712. Tel.: 512-232-1454; E-mail: jshear@mail.utexas.edu.

0006-3495/04/05/3223/07 $2.00

a single NIR photon, a process that enhances photoreaction efficiency. Action spectra for one-photon enhancement and two-photon excitation of product fluorescence are determined. In combination with previous results from electrophoretic analyses and cosolute studies, these results are used to construct a general model for the reaction process.

MATERIALS AND METHODS

Chemicals and materials

Sodium phosphate monohydrate, sodium citrate, sodium bicarbonate, sodium acetate, and sodium borate decahydrate were purchased from EM Scientific (Gibbstown, NJ). All other chemicals were purchased from Sigma Chemical (St. Louis, MO) and used as received. 5HT was purchased as its creatinine sulfate salt and analyzed at moderately low concentrations (between 20 and 300 μM) in pH 7 aqueous phosphate buffer. Water used to prepare buffers was purified by a Barnstead UV water system (Dubuque, IA), and all aqueous solutions were filtered with 0.2-μm pore size cellulose acetate syringe filters before use. Deoxygenation was accomplished by bubbling solutions within the sample cuvette with argon gas (Praxair, Danbury, CT; >99% purity), with flow rates adjusted so that steady-state visible emission generally was reached within 5 min. Signal stability was improved by terminating gas flow immediately before fluorescence data were acquired.

Multiphoton-excited fluorescence system

Coherent Mira 900 femtosecond modelocked titanium:sapphire (Ti:S) oscillators (Santa Clara, CA) were pumped by Coherent Verdi 5- or 10-W solid-state frequency-doubled Nd:vanadate lasers (532 nm) or an Innova 310 multiline argon ion laser. The detection system, which has been described previously (Gostkowski et al., 1998a, 2000), enabled simultaneous measurement of UV and visible fluorescence. In brief, the Ti:S laser beam was directed through the back aperture of a high numerical aperture (NA) microscope objective (Zeiss Fluar 100×, 1.3 NA, oil immersion, Jena, Germany). The objective focused excitation light through a No. 1.5 coverslip to a submicrometer-diameter focal spot within a solution reservoir. Fluorescence was collected by the objective and reflected from the laser beam path using long-pass UV- and visible-reflecting dichroic mirrors. Band-pass filters (UV channel) or a colored glass filter and a concentrated CuSO4 liquid filter (visible channel) were used to isolate fluorescence in the desired spectral ranges, and each channel was outfitted with a bialkali photomultiplier tube (Hamamatsu, HC125-02, Bridgewater, NJ) operated in photon-counting mode. Signal was measured using a dual-channel photon counter (Stanford Research Systems, model SR400, Palo Alto, CA) for steady-state measurements and a zero dead time multichannel scaler (Stanford Research Systems, model SR430) for nonsteady-state measurements.

Pump-probe experiments

Several pump-probe experiments were carried out in which two separate Ti:S focal volumes were spatially overlapped. Schematic representations of experimental designs used in these studies are shown in Fig. 1.

Fig. 1 *A* depicts a configuration used to investigate one-photon absorption at a variable delay time relative to a nonlinear-excitation event. Here, the output from a single Ti:S oscillator was divided at a polarizing beamsplitter (*PB1*), with the more intense portion focused into a single-mode optical fiber (0.16 NA, 4.3-μm inner diameter; Thor Labs, model FS-SC-4314, Newton, NJ) using a LOMO 0.22-NA microscope objective (Prospect Heights, IL). The relative orientation of the fiber and objective was manipulated using

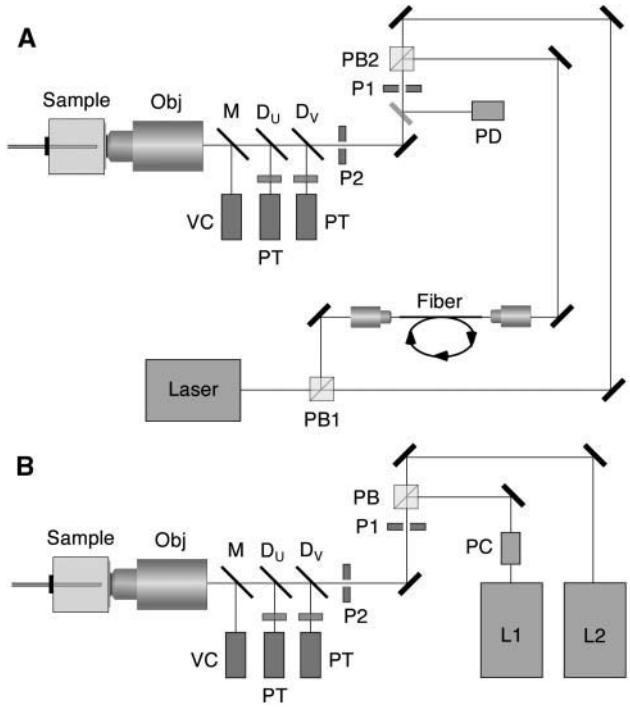

FIGURE 1 Experimental diagrams for pump-probe measurements in femtoliter focal volumes. (*A*) Single-laser instrument in which the titanium:sapphire output was split into two beams at polarizing beamsplitter PB1: one that retained a short pulse width and one that was temporally broadened using a 10 m optical fiber. The two beams were recombined at PB2 and aligned using a series of apertures (*P1* and *P2*) into a high NA microscope objective (*Obj*). The temporal relationship between the femtosecond and picosecond pulses was monitored using a fast photodiode (*PD*), and laser focal volumes were overlapped in solution by imaging reflections off the end face of a cut capillary (see text for full procedure). This process was monitored by directing the reflected light to a video camera (*VC*) using a mirror (*M*), which was removed before data was acquired. UV and visible fluorescence were reflected from the beam path using UV and visible dichroic mirrors (D_U and D_V, respectively), passed through spectral filters, and detected using photon-counting photomultiplier tubes (*PT*). (*B*) Configuration for two-laser (*L1* and *L2*) experiments. In some studies, a Pockel's cell (*PC*) was inserted into the beam path of a CW laser, providing a means to test nonsteady-state bleaching caused by low peak-intensity NIR light. For studies in which both lasers were modelocked, the Pockel's cell provided a means to briefly generate photoproduct with a high-intensity pulse train, which then was probed by a second, lower-intensity laser operating at an independent wavelength.

a commercially available alignment system (New Focus, model 9091, Santa Clara, CA). The length of the optical fiber (~10 m) was selected such that Mira pulses would be temporally broadened from ~150 fs to nearly 10 ps, thus dramatically reducing the efficiency of nonresonant multiphoton excitation and providing a means to study linear spectroscopic properties of reaction intermediates. This portion of the Ti:S output is referred to as the long pulse (LP) beam. A quarter-wave plate inserted into the beam path before the fiber coupler suppressed back reflections into the Ti:S laser cavity by preventing light from returning through PB1. The less intense portion of the beam split at PB1, the short pulse (SP) beam, was not subjected to highly dispersive elements and thus retained the capacity to efficiently excite multiphoton transitions. LP and SP beams were recombined at beamsplitter PB2 and were directed, co-linearly, into the fluorescence detection system described above. The temporal relationship between femtosecond and

picosecond pulses was measured using a fast photodiode and was controlled by varying the relative pathlengths of the LP and SP arms. In this instrument, which lacked pulse-picking capabilities, the maximal delay that could be achieved between the two pulses was ~13 ns (the inverse of the 76-MHz oscillator frequency).

In other experiments, a second Ti:S laser was used instead of splitting a single beam (Fig. 1 *B*), which allowed two lasers to be operated at different wavelengths. Here, the Ti:S cavity optics in one oscillator could be adjusted so that modelocking was not achieved, again dramatically reducing the capacity of this source to excite nonresonant multiphoton transitions. The output beams of the two lasers were combined at PB. In nonsteady-state bleaching studies, a Pockel's cell (Conoptics, model 350-50, Danbury, CT) controlled by a delay generator (Stanford Research Systems, DG 535, Sunnyvale, CA) was inserted into the continuous wave (CW) beam path, providing a means to test the effects of adding brief periods of CW NIR light to a continuous pulse train of modelocked light.

Alternately, the basic configuration in Fig. 1 *B* could be adapted so that both Ti:S lasers were modelocked, with the output of one directed into the Pockel's cell. In this way, photoproduct could be generated by one laser using a brief, high-intensity pulse train and probed by the second laser at a separate wavelength.

In the pump-probe configurations shown in Fig. 1, *A* and *B*, a requirement existed for spatially overlapping two high NA laser foci, a goal that was achieved by combining the two laser beams before the microscope objective. Because of the exceedingly small excitation volumes for multiphoton excitation (in these studies, $<1\ \mu m^3$), procedures for accurately and reproducibly aligning the two beams were essential. By positioning a polarizing beam combiner (polarizing beamsplitter *PB2*) ~200 cm from the sample, a relatively long distance was established in which small differences in beam overlap could be identified and eliminated. Alignment irises (pinholes *P1* and *P2*) were placed directly after the beam combiner and before the first dichroic mirror; the back aperture of the microscope objective served as a third alignment guide. With one beam fixed, alignment of the second beam was adjusted with a series of mirrors through the three apertures. Once approximate overlap was achieved visually, the two beam foci were positioned on the end surface of a fused silica capillary in the solution reservoir, producing two reflection spots in a procedure similar to that described previously (Gostkowski et al., 1998a). The laser spots then were translated to overlap using a video image to guide mirror adjustments, and the capillary was manipulated away from the focal plane before measurements were performed. Ultimately, overlap of the two foci was ensured by optimizing the superadditive effect on fluorescence signal generated from the two laser sources. Using this procedure, amplification of visible signal could be reproduced with a relative standard deviation of ~10%.

RESULTS

One-photon amplification of photoproduct generation

Reports by others suggested the possibility that excited-state absorption may be a common photodegradation mechanism when employing multiphoton excitation (Patterson and Piston, 2000; Chen et al., 2002). For various indoles, molecules populating S_1 potentially can undergo one-photon excitation to higher-energy singlet states, some of which are known to photoreact with high quantum yields (Steen, 1974; Kevan and Steen, 1975; Steen et al., 1976). To examine the possibility that such a pathway was involved in the generation of fluorescent 5HT photoproducts, the experimental system illustrated in Fig. 1 *A* was used. The Ti:S laser was operated at ~750 nm, a wavelength at which the SP beam focus was capable of generating excited-state 5HT (S_1- and potentially S_2-state molecules) via three-photon absorption with reasonable efficiency (Maiti et al., 1997). After excitation, molecules occupying S_1 (either through direct excitation or as a result of rapid internal conversion from higher states) decay according to the excited state lifetime of 5HT, ~3.8 ns (Chattopadhyay et al., 1996). The LP pulse width (Δt) was broadened by traversing a 10-m segment of optical fiber, which was estimated to yield a full-width half maximal pulse width of between 5 and 10 ps (C. Xu, Cornell University, personal communication, 2003). Because the absorption probability for an *n*-photon process (in the absence of saturation) scales as $\Delta t^{(1-n)}$ (Xu and Webb, 1996; Maiti et al., 1997), any significant increase in signal created by overlapping the broadened pulse with the femtosecond pulse would be expected to result only from 1PE. The LP beam was confirmed to have essentially no capacity to excite nonlinear transitions.

Amplification of visible emission using 1.2- and 12.2-ns delay times is shown in Fig. 2. Within experimental uncertainty ($N = 3$, relative standard deviation $\approx$ 35%), the visible emission at these delay times was indistinguishable. Because the S_1-state population is expected to decrease from ~70% of maximum at 1.2 ns to <5% at 12.2 ns, it is clear that the species undergoing 1PE must have a substantially longer lifetime than S_1-state 5HT.

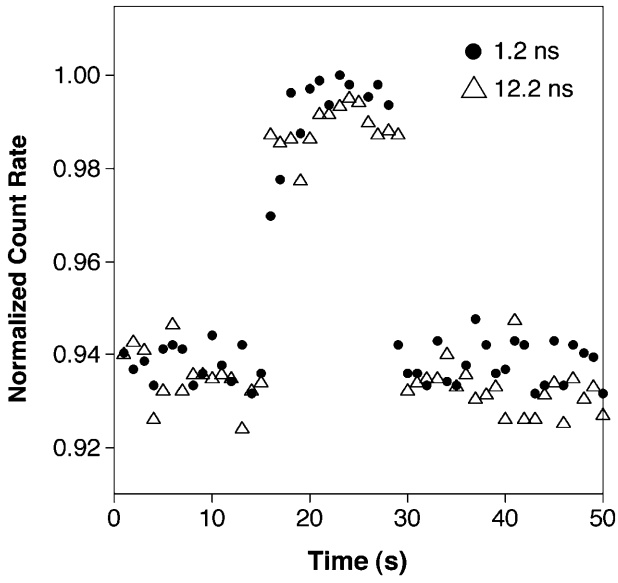

FIGUR E 2 Effect of temporally broadened laser pulses on the production of steady-state visible emission from 5HT at short (*1.2 ns*) and long (*12.2 ns*) delay times relative to femtosecond pulses. From ~15 to 30 s, a train of temporally broadened (5–10 ps) pulses (20-mW time-averaged power) was allowed to interact with a volume of 5HT solution already subjected to a train of modelocked (~150 fs) pulses (50-mW time-averaged power). A high-intensity (single point) data spike was removed from the 1.2-ns plot for clarity of presentation. Laser wavelength $\approx$ 750 nm.

To evaluate the wavelength dependence of the 1PE amplification effect, two independent Ti:S lasers were used (configuration shown in Fig. 1 *B*), with one laser modelocked and the other operated in a CW mode at intensities insufficient to generate measurable nonlinear excitation. This approach sacrificed temporal information but allowed significantly greater powers to be used for 1PE amplification than were possible in the pulse-delay experiments described above, thus providing a more quantitative and reproducible analysis system.

Amplification of visible signal scaled linearly with CW laser power up to several hundred milliwatts, with photoproduct emission nearly doubling at 600 mW. To examine the possibility that these enhancements were caused by solution heating (expected to be no more than several degrees Celsius; Schönle and Hell, 1998), visible emission was measured from a 5HT solution at temperatures up to 70°C using a single, tightly focused femtosecond Ti:S beam at various wavelengths. No significant enhancements in emission were observed.

Importantly, application of CW light also caused a decrease in UV emission, a result most likely indicative of an increased photobleaching rate. This conclusion is supported by nonsteady-state experiments in which nonlinear (and linear) excitation steps were promoted by a modelocked beam, and the intensity of a second, CW beam was switched high for microsecond to millisecond periods to enhance one-photon transition rates. UV fluorescence was suppressed after application of CW light, but recovered to the pre-transient baseline level over hundreds of microseconds, a timescale indicative of 5HT diffusional replenishment into a high NA multiphoton focal volume (Brown et al., 1999).

The wavelength dependence of one-photon action cross sections for visible-emission amplification was investigated by tuning the CW Ti:S output over wavelengths ranging from 717 to 873 nm. Spectra were acquired under conditions in which amplification scaled essentially linearly with CW laser power and fractional UV photobleaching was minor. To ensure that data was not skewed by artifacts related to the choice of pump wavelength (for example, a changing spatial overlap of pump and probe foci), data were acquired with the modelocked laser tuned to more than one wavelength (Fig. 3 *A*). The efficiency of one-photon amplification was observed to decrease approximately fivefold over the examined wavelength range.

Although suppression of UV fluorescence by CW light also decreases at long wavelengths (data not shown), the one-photon bleaching spectrum is qualitatively and quantitatively distinct from the visible-amplification spectrum: a maximum exists between 750 and 800 nm, and cross sections change by $<20\%$ from $\sim$720 to 920 nm. These results indicate that multiple processes or states may be effected by one-photon excitation of excited-state 5HT.

We previously have reported that large enhancements in photoproduct visible emission accompany deoxygenation of low concentration 5HT solutions in various non-Good's buffer systems (Gostkowski et al., 2000). Because photoproduct excited-state lifetimes are short ($\sim$0.8 ns), this result implied the existence of a relatively long-lived intermediate in the photoreaction pathway whose lifetime depends strongly on the presence of molecular oxygen (or oxygen-derived species). Under ambient molecular oxygen concen-

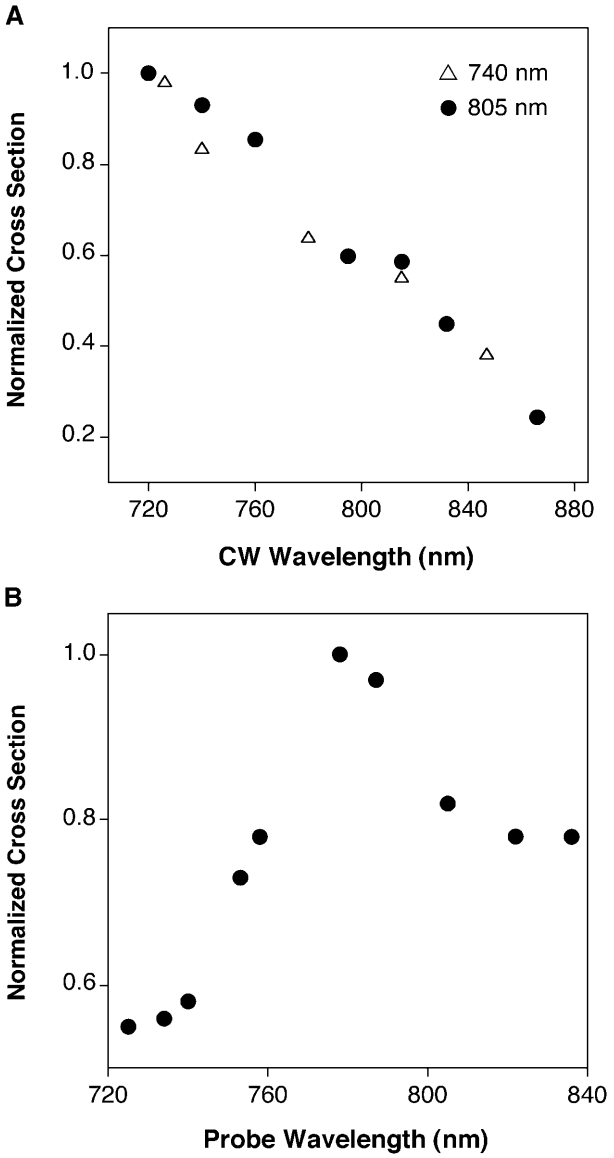

FIGURE 3 (*A*) Relative one-photon action cross sections for amplification of visible emission measured using modelocked wavelengths of 740 nm (△) and 805 nm (●). Data taken using 750-nm modelocked light showed a similar trend with somewhat greater data scatter. (*B*) Relative two-photon action cross sections for excitation of visible emission from 5HT photoproduct. The L1 laser (Fig. 1), maintained at 807 nm for these studies, was used to transiently create photoproduct when the Pockel's cell was switched to a high throughput state for $\sim$3 ms. After this beam was switched back to low power, photoproduct fluorescence was probed using the (overlapped) focus from the L2 beam during the diffusional escape period. Measurements were made over thousands of repeat transients.

trations, an intermediate that is highly sensitive to oxygen would be expected to persist for a minimum of $\sim 10^{-7}$ s (assuming a quenching constant of $\leq 10^{10}$ M^{-1} s^{-1}).

In these studies, we investigated the possibility that one-photon excited-state absorption occurs from this oxygen-sensitive state by measuring the dependence of signal amplification on CW laser power in the presence and absence of molecular oxygen. As the intensity of CW light is increased, a regime should be reached where one-photon absorption probability approaches unity (observed as signal saturation); in the simplest case, the laser power needed to reach saturating conditions should scale inversely with the intermediate-state lifetime. When corrected for ground-state 5HT depletion, amplification of visible emission in de-oxygenated 5HT solutions scaled linearly with CW input for powers as large as several hundred milliwatts. In the presence of oxygen, the laser intensity at which visible-amplification deviated from linearity increased only by approximately twofold, suggesting that one-photon excitation takes place from an intermediate that is not highly oxygen sensitive. Based on the focal point intensity required to approach saturation ($\sim 10^{27}$ photons s^{-1} cm^{-2}) and a lifetime significantly $>10^{-8}$ s, one-photon action cross sections for visible amplification are calculated to be $<\sim 10^{-19}$ cm^2. This simple, order of magnitude estimate assumes a constant CW intensity throughout the three-photon excitation volume and is based on an approximate twofold decrease in the instantaneous slope of amplification versus CW laser power at 1 W power. A caveat to this estimate would arise if the visible-emitting photoproduct also were capable of undergoing one-photon-enhanced bleaching, a possibility that should be assessed in future studies.

Two-photon fluorescence action spectrum of 5HT photoproduct

Previous experiments showed that visible emission from the multiphoton-generated 5HT photoproduct is excited by absorption of two NIR photons (Shear et al., 1997). However, because a single laser was used both to generate and detect photoproduct, the wavelength dependencies of the two processes were convolved. By modelocking both Ti:S lasers in Fig. 1 *B*, it was possible to specifically investigate the spectroscopic properties of the 5HT photoproduct. Here, the beam passing through the Pockel's cell (from the first laser, *L1*) was switched to a high photoreaction power (275 mW) for several milliseconds, then returned to a nominally off state (a power at which generation and excitation of photoproduct was negligible). The second laser (*L2*) was maintained at a constant power (65 mW) throughout the procedure and was used to probe fluorescence in the period immediately after the L1 beam was switched low (i.e., during the initial several hundred microseconds over which photoproduct diffused into bulk solution). The intensity of L2 was chosen to be low enough so that it produced little additional photoproduct and that visible emission scaled approximately as the square of the laser intensity, but high enough to probe existing photoproduct with reasonable efficiency. Fig. 3 *B* shows relative two-photon fluorescence action cross sections measured for L2 wavelengths between 725 and 836 nm. Fluorescence was measured from a reference solution of fluorescein under conditions of low fractional bleaching to provide a means for correcting 5HT signal for differences in laser temporal pulse widths and optical throughput values at different excitation wavelengths.

DISCUSSION

Measurements of 5HT visible emission have been made in the presence of various cosolutes, offering additional clues regarding photoreaction mechanisms. We have reported that the presence of different pH buffers can have large effects on 5HT photoproduct visible emission and concentration scaling (Shear et al., 1997; Gostkowski et al., 2000). HEPES and other Good's buffers, for example, support substantially higher photoproduct emission than phosphate buffer at low 5HT concentrations, although these differences are minor at concentrations greater than several millimolar. Because the photoproduct excited-state lifetime is indistinguishable in HEPES and phosphate (Gostkowski et al., 2000), these results suggest that buffer identity can affect the photoproduct formation efficiency. Importantly, visible photoproduct signal can be >10-fold higher in HEPES than in phosphate even under conditions in which the total 5HT UV photobleaching rate is greater in phosphate. It thus appears that multiple photobleaching branches exist and are preferentially accessed depending on the particular solution (and excitation) conditions.

A second relevant finding was that photoproduct signal increases approximately linearly with 5HT concentration in Good's buffers but scales superlinearly in phosphate (signal $\sim[5HT]^{1.3}$). When molecular oxygen was excluded from phosphate buffer, nearly linear concentration scaling was observed for relatively low 5HT concentrations, and the overall fluorescence signal approached that achieved in HEPES. Together, these results suggest that formation of visible photoproduct can be strongly inhibited by an oxygen species, and that various cosolutes (including HEPES and additional 5HT molecules) may in some manner protect a reaction intermediate against quenching by oxygen.

As described above, one-photon absorption enhances photoproduct formation while depleting ground-state 5HT population: under conditions in which photoproduct signal was increased nearly twofold, steady-state UV fluorescence decreased by more than 25%. Enhanced photobleaching indicates that an intermediate capable of absorbing CW light retains the potential to relax to S_0-state 5HT (i.e., the intermediate has not committed to any photoreaction pathway). However, the fact that one-photon UV-photobleaching and visible-amplification spectra are not identical implies that

multiple one-photon bleaching pathways may exist. A primary route for one-photon-enhanced photobleaching may be $S_1 \rightarrow S_2$ excitation, a transition expected to enhance photobleaching efficiency and whose energy coincides well with the NIR wavelengths used in these studies. With improvements in signal/noise, the possibility of $S_1 \rightarrow S_2$ excitation could be assessed further by determining one-photon enhanced photobleaching as a function of femtosecond–picosecond pulse delay time.

In contrast, the presence of molecular oxygen in 5HT solutions has only minor effects on UV emission, even under conditions in which deoxygenation results in a large amplification of visible emission. It therefore appears likely that quenching of the reaction by oxygen does not replenish ground-state 5HT, but instead leads to nonfluorescent (dark) photoproducts.

Fig. 4 proposes photoreaction mechanisms consistent with our various results. Based on these studies, it appears most likely that two separate intermediates exist in the pathway to the visible-emitting product: 1), an initial one-photon excitable state with a lifetime significantly longer than 12 ns that interacts modestly with an oxygen-related species and that may be able to regenerate ground-state 5HT and 2), a subsequent intermediate that persists long enough ($>10^{-7}$ s) to be effected strongly by an oxygen species and that does not appear capable of reforming ground-state 5HT. Note that two possible one-photon pathways for dark-product formation are shown (one from the S_1 state and one from the first intermediate), both of which are consistent with current results.

Effects of various solution additives suggest that radicals play a role in the production of visible emission from 5HT solutions, although these results do not yet indicate a conclusive mechanism. For example, 10 mM mercaptoethylamine, a general radical quencher, was found to enhance steady-state 5HT UV fluorescence and significantly suppress visible emission at high excitation intensities, whereas 20 mM diazylbicyclooctane, a singlet oxygen quencher, amplified both UV and visible emission. Nitrous oxide (N_2O), a commonly used scavenger for hydrated electrons (Jovanovic and Steenken, 1992), decreased visible emission. Although these cosolutes were present at too low a concentration to collisionally deactivate the fluorescent state of the 5HT photoproduct, these steady-state results may represent a convolution of changes in the efficiency of formation and degradation of fluorescent photoproduct. More specific conclusions regarding the effects of cosolutes would be possible through time-resolved experiments.

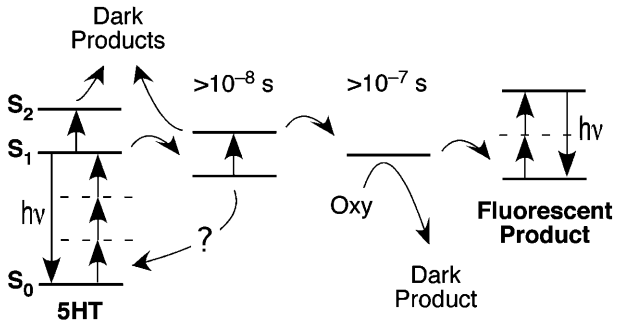

FIGURE 4 Proposed pathway for generation of fluorescent 5HT photoproduct.

Electrophoretic analyses have been performed to gain additional insights into the molecular characteristics of the visible-emitting 5HT photoproduct (Gordon et al., 2001; Plenert and Shear, 2003). Because this species can degrade via thermal pathways within tens to hundreds of milliseconds of its formation, we developed a means to perform multiphoton photoreaction and analysis in the presence of large electrophoretic fields. By using fields that ranged from $\sim 10^3$ to 10^5 V cm^{-1}, photoproducts could be transported over short capillary segments ($\sim 10\ \mu$m) within microseconds to milliseconds of their formation with separation efficiencies sufficient to resolve species generated from different hydroxyindoles. On this timescale, no significant changes in electrophoretic mobility were observed after photoreaction. Moreover, electrophoretic studies on hydroxyindole-reaction mixtures (5HT and either the neutral 5HTrp or the anionic 5-hydroxyindole-3-acetic acid, 5-hydroxyindole-3-acetic acid) reveal the same products as reactions performed on single-component solutions, discounting the possibility that dimerization reactions are responsible for formation of visible-emitting hydroxyindole photoproducts.

These results demonstrate that the 5HT visible-emitting photoproduct has the same charge, and an experimentally indistinguishable frictional drag coefficient, as its parent hydroxyindole, a relatively surprising result in light of the large differences in excitation and emission properties of 5HT and its fluorescent photoproduct. Moreover, the ability of disparate 5-hydroxyindoles, including 5HT, 5HTrp, 5-hydroxyindole-3-acetic acid, 5-hydroxyindole-2-carboxylic acid, and 5-hydroxyindole, to form visible-emitting photoproducts is evidence that ring-forming events are not necessary to these photoreactions. These findings, and the similarity of photoproduct excitation energies to one-photon 5-indoxyl-radical spectra, suggested that relatively long-lived radicals could be responsible for multiphoton-excited visible emission (Gordon et al., 2001). This possibility recently was investigated for 5HTrp (Bisby et al., 2003), whose multiphoton-derived fluorescent photoproduct produced a transient absorption spectrum similar to that of the indoxyl radical. Notably, however, the presence of ascorbate as a cosolute had little effect on visible emission, despite its demonstrated capacity to act as a strong reductant for the indoxyl radical. Bisby also identified a strongly acidic site (apparent $pK_a \approx 1$) by measuring the excited-state lifetime of the visible-emitting product as a function of pH.

The chemical processes leading to creation of visible-emitting photoproducts via multiphoton excitation of

5-hydroxyindoles are clearly complex and remain inconclusive. Given the modest oxygen sensitivity of one-photon-amplified photoproduct generation, the possibility must be considered that the CW-sensitive intermediate is the T_1 state of 5HT. Transient absorption measurements of T_1-state 5HT and detailed calculations of the 5HT excited-state electronic structure may provide additional insights into this process. In addition, the possibility that 308-nm excitation yields the same product as NIR multiphoton excitation would provide an opportunity for studies that could conclusively identify the fluorescent photoproduct. Rapid electrospray coupling of UV-excited photochemical products into a mass spectrometer, for example, may identify minor changes in molecular mass that were beyond the resolving capabilities of our electrophoretic analyses.

Finally, it is interesting to note that there is significant overlap in the spectra for three-photon excitation of 5HT (Maiti et al., 1997), one-photon excitation of the reaction intermediate, and two-photon excitation of fluorescent photoproduct. Were this not the case, it would not be feasible to excite all processes with a single Ti:S oscillator, and the initial observation of multiphoton-excited photoproduct generation may not have been made. Such a conclusion raises the intriguing possibility that multistep photoderivatization reactions may be possible for other compounds given the appropriate photonic control.

We thank Chris Xu for group velocity dispersion calculations on fiber-broadened pulses.

Support for these studies from the National Science Foundation (grant 0317032) and the Welch Foundation (grant F-1331) is gratefully acknowledged.

REFERENCES

Bisby, R. H., M. Arvanitidis, S. W. Botchway, I. P. Clark, A. W. Parker, and D. Tobin. 2003. Investigation of multiphoton-induced fluorescence from solutions of 5-hydroxytryptophan. *Photochem. Photobiol. Sci.* 2:157–162.

Brown, E. B., E. S. Wu, W. Zipfel, and W. W. Webb. 1999. Measurement of molecular diffusion in solution by multiphoton fluorescence photobleaching recovery. *Biophys. J.* 77:2837–2849.

Chattopadhyay, A., R. Rukmini, and S. Mukherjee. 1996. Photophysics of a neurotransmitter: ionization and spectroscopic properties of serotonin. *Biophys. J.* 71:1952–1960.

Chen, T.-S., S.-Q. Zeng, Q.-M. Luo, Z.-H. Zhang, and W. Zhou. 2002. High-order photobleaching of green fluorescent protein inside cells in two-photon excitation microscopy. *Biochem. Biophys. Res. Commun.* 291:1272–1275.

Gordon, M. J., E. Okerberg, M. L. Gostkowski, and J. B. Shear. 2001. Electrophoretic characterization of transient photochemical reaction products. *J. Am. Chem. Soc.* 123:10780–10781.

Gordon, M. J., and J. B. Shear. 2001. Electrophoretic characterization of dynamic biochemical microenvironments. *J. Am. Chem. Soc.* 123:1790–1791.

Gostkowski, M. L., T. Curey, E. Okerberg, T. Kang, D. A. Vanden Bout, and J. B. Shear. 2000. Effects of molecular oxygen on multiphoton-excited photochemical analysis of hydroxyindoles. *Anal. Chem.* 72:3821–3825.

Gostkowski, M. L., J. B. McDoniel, J. Wei, T. E. Curey, and J. B. Shear. 1998a. Characterizing spectrally diverse biological chromophores using capillary electrophoresis with multiphoton-excited fluorescence. *J. Am. Chem. Soc.* 120:18–22.

Gostkowski, M. L., J. Wei, and J. B. Shear. 1998b. Measurements of serotonin and related indoles using capillary electrophoresis with multiphoton-excited hyperluminescence. *Anal. Biochem.* 260:244–250.

Jovanovic, S. V., and S. Steenken. 1992. Substituent effects on the spectral, acid-base, and redox properties of indolyl radicals: a pulse radiolysis study. *J. Phys. Chem.* 96:6674–6679.

Kevan, L., and H. B. Steen. 1975. Polarity effects on wavelength dependence of the fluorescence quantum yield for indole. *Chem. Phys. Lett.* 34:184–188.

Maiti, S., J. B. Shear, W. R. Zipfel, R. M. Williams, and W. W. Webb. 1997. Measuring serotonin distribution in live cells with three-photon excitation. *Science.* 275:530–532.

Patterson, G. H., and D. W. Piston. 2000. Photobleaching in two-photon excitation microscopy. *Biophys. J.* 78:2159–2162.

Plenert, M. L., and J. B. Shear. 2003. Microsecond electrophoresis. *Proc. Natl. Acad. Sci. USA.* 100:3853–3857.

Schönle, A., and S. W. Hell. 1998. Heating by absorption in the focus of an objective lens. *Opt. Lett.* 23:325–327.

Shear, J. B., C. Xu, and W. W. Webb. 1997. Multiphoton-excited visible emission from serotonin solutions. *Photochem. Photobiol.* 65:931–936.

Springer, G. H., and D. A. Higgins. 2000. Multiphoton-excited fluorescence imaging and photochemical modification of dye-doped polystyrene microsphere arrays. *Chem. Mater.* 12:1372–1377.

Steen, H. B. 1974. Wavelength dependence of the quantum yield of fluorescence and photoionization of indoles. *J. Chem. Phys.* 61:3997–4002.

Steen, H. B., M. K. Bowman, and L. Kevan. 1976. Temperature dependence of a process competing with S2–S1 internal conversion in indole and phenol in aqueous solutions. *J. Phys. Chem.* 80:482–486.

Xu, C., and W. W. Webb. 1996. Measurement of two-photon excitation cross sections of molecular fluorophores with data from 690 to 1050 nm. *J. Opt. Soc. Am. B.* 13:481–491.